

# Criteria for room temperature topological transport

Matthew Brahlek<sup>1\*</sup>

<sup>1</sup>Materials Science and Technology Division, Oak Ridge National Laboratory, Oak Ridge, TN, 37831, USA

Correspondence should be addressed to \*brahlekm@ornl.gov

**Abstract:** It is often quoted that novel electronic devices based on topological states can operate at room temperature, but empirically it is not clear if this is truly possible. Here we develop simple criteria for the maximum temperature at which the topological surface states or edge states could dominate the electrical transport properties, a necessity for a topological device. This is demonstrated for 3-dimensional topological insulators (TIs) and 1D quantum anomalous Hall insulators (QAHIs), though this can be applied to similar systems. The density of thermally activated carriers gives the upper temperature when topological surfaces may dominate transport. By considering the space of band gap, dielectric constant, and effective mass, a clear boundary emerges that separates current TI materials from those that may operate at or above room temperature, and, thus, providing clear criteria to search for next-generation materials. For QAHIs, current materials are also far from the room temperature limit, but liquid nitrogen temperatures may be within reach, especially considering heterostructures with magnetic materials. Establishing these specific criteria is crucial to design new materials systems, which is key to pushing into a new generation of topological technologies.

Key Words: topological, topological insulator, quantum anomalous Hall, topological materials, quantum materials

This manuscript has been authored by UT-Battelle, LLC under Contract No. DE-AC05-00OR22725 with the U.S. Department of Energy. The United States Government retains and the publisher, by accepting the article for publication, acknowledges that the United States Government retains a non-exclusive, paid-up, irrevocable, world-wide license to publish or reproduce the published form of this manuscript, or allow others to do so, for United States Government purposes. The Department of Energy will provide public access to these results of federally sponsored research in accordance with the DOE Public Access Plan (<http://energy.gov/downloads/doe-public-access-plan>).

Topology is a very general notion used to broadly classify objects, and has been extensively used in condensed matter physics to describe many systems including, the relevant system of the current work, topological band structures<sup>1,2</sup>. These range from the 1-dimensional (1D) states that exist on the boundary of a 2-dimensional (2D) insulator such as the quantum Hall insulator (QHI)<sup>3,4</sup>, to the quantum spin Hall phase<sup>5,6</sup>, and quantum anomalous Hall insulator (QAHI)<sup>7-10</sup>, and the 2D Dirac-like topological surface states (TSS) that exist on the surfaces of 3D topological insulators (TIs)<sup>11</sup>. Together the novel character of topological materials make them of interest for a wide range of fundamental studies and many applications in areas ranging from quantum computation to spintronics<sup>12-14</sup>. However, one of the major challenges is that they are rarely true insulators—their 2D or 3D bulk states are nearly ubiquitously metallic, which acts as a parallel conduction channel that electrically shorts the transport through the topological states.

This challenge of parallel conduction is chemically rooted in the same fundamental reason why they are topological and profoundly impacts the maximum temperature where the topological states may dominate the transport. The  $Z_2$  topological number becomes non-trivial if the bulk conduction and valence bands are inverted due to strong spin-orbit coupling. This requires narrow band gaps, where spin-orbit coupling, which, in a broad sense is relatively weak compared the Coulombic interaction responsible for chemical bonding and bandgap formation, is sufficiently strong to invert the orbital character of the conduction and valence bands. Following Cava et al.<sup>15</sup>, this requirement is fulfilled when the constituent elements have similar electronegativity, giving rise to a strong covalency. This means that both the bandgap will be narrow and charged antisite defects will have a low formation energy, and, therefore, are likely to occur with a high density. The key materials that have dominated the field over the past decade are the tetradymite 3D TIs  $\text{Bi}_2\text{Se}_3$ ,  $\text{Bi}_2\text{Te}_3$ , and  $\text{Sb}_2\text{Te}_3$ <sup>15,16</sup>, and it has proven a major challenge to both understand and mitigate defects sufficiently to achieve a true topological insulating phase from transport<sup>17-21</sup>. However, the caveat arises that this true insulating phase for both TIs, as well as QAHIs, occurs at very low temperatures near absolute zero, often requiring dilution refrigerators operating at sub-Kelvin temperatures. This is a challenge for many researchers to probe these states as well as precluding or hampering any technological applications. Here, we show that the bandgap, dielectric constant, effective mass, and the defect density set the relevant temperature scales for where the TSS or TES dominate the electronic response of a material. This is obtained by combining the Mott criterion for critical carrier density that governs when a 3D insulator becomes metallic, and the temperature dependence of thermally activated carriers; for the case of the QAHI we compare the sheet resistance to the resistance quanta. Beyond these examples, this is broadly applicable and provides well-defined bounds in temperature for where novel transport properties can be observed. These parameters are fundamentally tied to key aspects of the materials chemistry, which will serve as a guide to find new materials that will enable room temperature topological devices.

The Mott-criterion gives the critical density of carriers to push an insulator into a metal phase. When a dopant atom is inserted into an insulator, its associated charge is screened by polarizing the surrounding atoms in the lattice. This screening follows a hydrogen-like potential, which is rescaled due to the dielectric response of the material. This yields an effective rescaled Bohr radius given by  $a = \epsilon(m_e/m^*)a_B$  where  $m_e$  is the free electron mass,  $m^*$  is the effective mass,  $\epsilon$  is the dielectric constant, and  $a_B$  is the free-space Bohr radius which is about 0.5 Å. The Mott-criterion predicts that when atoms are doped into a material with a sufficient density,  $N_D$ , then the insulator becomes metallic. This critical density is given by  $N_D \approx (0.26/a)^3$ <sup>22</sup>. For the tetradymite TIs (Bi<sub>2</sub>Se<sub>3</sub>, Bi<sub>2</sub>Te<sub>3</sub>, and Sb<sub>2</sub>Te<sub>3</sub>) the dielectric constants are relatively large, ~100-200, and the effective masses are relatively small, ~0.1 $m_e$ <sup>16</sup>. This yields a relatively low  $N_D \approx 10^{14}$ - $10^{15}$  cm<sup>-3</sup><sup>16,19</sup>. In contrast, for semiconductor materials like Si the critical density is orders-of-magnitudes larger at around  $10^{17}$ - $10^{18}$  cm<sup>-3</sup><sup>22</sup>. Finite disorder, due to effects such as Anderson localization, however, aid the suppression of these bulk states, as captured by Ioffe-Regel criterion where  $k_F l \sim 1$ , where  $k_F$  is the Fermi wave vector and  $l$  is the mean-free-path, which will push the insulator to metal transition to higher density<sup>19</sup>; therefore,  $N_D$  is taken to be  $10^{15}$  cm<sup>-3</sup> for the tetradymite TIs.

Establishing an upper limit on the temperature scale for transport to be dominated by a topological state requires calculating the number of thermally induced free carriers and comparing that to the Mott criterion for a 3D TI and the resistance quantum for the QAHI. If a minimal density of charged defects is incorporated into a material during growth such that the Fermi level,  $E_F$ , is located inside the bandgap, then the material is in the intrinsic limit. This establishes the upper limit for temperature. Finite temperature will then cause a finite number of carriers to be excited across the bulk band gap. The number density is then given by

$$(1) \quad N(T) = \int D(E)f(E, T)dE,$$

where  $D(E)$  is the density of states and

$$(2) \quad f(E, T) = \frac{1}{1+e^{E/(k_B T)}}$$

is the Fermi function, where  $E$  is the energy,  $T$  the temperature and  $k_B$  is Boltzmann's constant. For quadratically dispersing bands, the density of states per volume relative to the center of the band gap is given by

$$(3) \quad D_{3D,i}(E) = \frac{g}{4\pi^2} \left(\frac{2m_i^*}{\hbar^2}\right)^{3/2} \sqrt{E - \frac{E_g}{2}}$$

in 3D, and by

$$(4) \quad D_{2D,i}(E) = \frac{gm_i^*}{2\pi\hbar^2}$$

in 2D. Here,  $g$  is the spin degeneracy ( $g = 2$  for a spin degenerate band and 1 for a gapped TSS),  $\hbar$  is Planck's reduced constant, and the subscript  $i$  indicates if the band is an electron ( $n$ ) or hole ( $p$ ). For the 3D case the number of excited carriers can be calculated by evaluating the following integral:

$$(5) \quad N_{3D}(T) = \int_{-\infty}^{-\frac{E_G}{2}} D_{3D,p}(E) f(E, T) dE + \int_{\frac{E_G}{2}}^{\infty} D_{3D,n}(E) f(E, T) dE$$

for 3D, and

$$(6) \quad N_{2D}(T) = \int_{-\infty}^{-\frac{E_G}{2}} D_{2D,p}(E) f(E, T) dE + \int_{\frac{E_G}{2}}^{\infty} D_{2D,n}(E) f(E, T) dE$$

in 2D. This gives the number of free electrons, and, although simple, can give a first order estimation on the bounds where the topological states dominate the transport processes. It is worth noting that this does not account for differences among the effective masses of the valence and conduction bands and ignoring shifts of the band gap versus temperature<sup>23</sup>. As schematically shown in Figure 1a, topological band structures are characterized by band gaps, with a lower dimensional state within this gap: For a 3D TI with a bandgap  $E_G$ , the gap is spanned by 2D Dirac like TSS. If the 2D TSS can be gapped,  $\Delta$ , via breaking, for example, time reversal symmetry, this can give rise to a linear 1D chiral edge state characteristic of the QAHI. As such, the integrals in equation (5) and (6) can be evaluated across a range of realistic materials parameters to understand the bounds on temperature for observing transport effects dominated by these novel states. First, the case of 3D TIs is discussed, followed by the case of a gapped TSS and the associated QAHI.

The integrals in equation (5) and (6) are evaluated numerically. Although closed solutions for both (5) and (6) likely can be found with some limiting assumptions (e.g.  $E \gg k_B T$  reduces Fermi statistics to Boltzmann statistics and (5) has a closed solution in terms of gamma functions and (6) can be directly integrated), numerical solutions were deemed sufficient since the number and range of realistic parameters is small. The free parameters for the integral are the band gap, and the effective mass. As mentioned above, the current host of topological materials are typically in the range of  $m^* \approx 0.1m_e$  with bandgaps less than about 0.3 eV (see Ref. <sup>24</sup> for a thorough list of known and predicted TIs). Eq. (5) was evaluated numerically, and, as shown in Figure 2a, the resulting  $N_{3D}$  curves were plotted as a function of temperature for  $m^* \approx 0.1m_e$  with band gaps ranging from 0.01-1.1 eV. (For consistency, it is noted that these results agree well with Ge ( $E_G = 0.7$  eV,  $m_e^* = 0.6m_e$  and  $m_h^* = 0.3m_h$ ) and Si ( $E_G = 1.1$  eV,  $m_e^* = 1.0m_e$ ,  $m_h^* = 1.0m_h$ ) that have intrinsic carrier densities at room temperature of  $N_{3D,Ge} \approx 2 \times 10^{13} \text{ cm}^{-3}$ , and  $N_{3D,Si} \approx 1 \times 10^{10} \text{ cm}^{-3}$  <sup>23</sup>, which are sufficiently close to the results in Figure 2a, considering the electron and hole effective masses are larger than those used in Figure 2a.) From this calculation, the number of free carriers ubiquitously increases with increasing temperature with the lowest band gap having the steepest increase, as expected. For comparison the estimation of the Mott criterion of  $N_D \approx 10^{15} \text{ cm}^{-3}$  was plotted as a dashed gray horizontal line. The

intersection of the thermally-excited carrier density curves with the horizontal line  $N_D$ , gives an estimation when bulk conduction will arise and will be substantial enough to obscure transport through the TSS. The temperatures where the intersections occurred were found and plotted versus band gap in Figure 2b. Since  $m^*$  is an additional parameter, similar calculations were performed for effective masses from 0.1 to  $1.0m_e$ .

The important result of these calculations for a 3D TI is that at typical band gaps for TIs ( $<0.3$  eV) transport through the bulk state is expected to contribute to the overall conduction for temperatures around 100-150 K, and, therefore, transport cannot be dominated by the TSS near room temperature. This, however, does not preclude topological phenomena at room temperature, and, in fact, points to the key parameters that must be modified to achieve this. As can be seen in Figure 2b, there is a near linear relation among the temperature where the bulk states will start contributing to the transport and bandgap. Therefore, for every 0.1 eV increase in band gap the upper temperature will increase by roughly 50 K. Also, plotted in Figure 2b are curves for various effective masses ranging from 0.1- $1.0m_e$ . Here, there is a weak dependence on  $m^*$ —in going from 0.1 to  $1.0m_e$  attains a change of about 15-20% in temperature (concerning  $m^*$  alone, the dominant behavior is likely opposite this, as discussed next.). The Mott criterion depends on both the dielectric constant as well as the effective mass, via  $N_D \propto (m^*/\epsilon)^3$ . Therefore, changing either of these effectively changes the temperature at which the bulk states will start to conduct; since  $N_D$  depends cubically on  $m^*/\epsilon$ , this can be very effective at raising the upper temperature. For example, the green curve shown in Figure 2b was calculated with  $N_D = 10^{16} \text{ cm}^{-3}$ , with  $m^* = 0.1m_e$ , which corresponds  $\epsilon \rightarrow (1/10)^{1/3}\epsilon$ , a 50% reduction in  $\epsilon$ . This significantly raises the critical temperature, which shows that, given the scale of typical bandgaps for TIs, can be attained by reducing the dielectric constant (or to a lesser extent increasing the effective mass). To explicitly demonstrate the parameter space necessary to isolate the transport through the TSS at room temperature, the value of  $N_{3D}$  at  $T = 300$  K was equated to the functional form of  $N_D$ , which enabled solving for the dielectric constant for a given effective mass and band gap; this sets the maximum dielectric constant  $\epsilon_{max}$  where transport through the TSS can be isolated at room temperature (i.e.  $\epsilon < \epsilon_{max}$ , else bulk states can conduct in parallel). These curves,  $\epsilon_{max}$  vs  $E_G$ , are plotted in Figure 2c for various  $m^*$  as solid lines, which form a tight band that separates ideal from non-ideal materials, where the bulk state will conduct at room temperature. This plot also includes data from many known TI materials. In fact, only a few of the materials predicted to be TIs have been sufficiently well characterized to be included in this plot. Figure 2c shows that all materials sit well above the  $\epsilon_{max}$  vs  $E_G$  indicating none are suitable for room temperature operation. This highlights that new materials are necessary, and a basic strategy to find these is discussed below.

Now we move onto the case of the QAHI by numerically evaluating eq. (6), where the 3D bandgap is replaced by the 2D magnetic gap  $\Delta$ , and the spin degeneracy term is taken to be  $g = 1$ , reflecting the spin polarized TSS. The results are plotted for effective masses equal to  $0.1m_e$  and  $0.2m_e$  in Figure 3a-b,

respectively for various magnetic gaps ranging from 0.01-0.4 eV. One challenge arises for the case of 2D in comparison to the previous case of 3D: scaling theory predicts that all 2D system should be localized<sup>25</sup>. This precludes the establishment of an analogy to the Mott-criterion. Rather, for comparison to the quantized resistance expected for the QAHI, a range of carrier densities were considered and the corresponding resistances relative to the quantum of resistance was estimated. A mobility of order  $2000 \text{ cm}^2\text{V}^{-1}\text{s}^{-1}$ , which is typical of TSS<sup>17,18,20,26</sup> and a carrier density around  $N_{2D} = 10^{10} \text{ cm}^{-2}$  correspond to roughly  $10 \times h/e^2$ , and, therefore, perfect quantization would be obscured by about 10%. Similarly,  $10^{11} \text{ cm}^{-2}$  corresponds to roughly  $1 \times h/e^2$ , which, for practical purposes, would wash out any signature of quantized transport. Contrary to the expectation that higher mobility is better, samples with larger mobility would have a lower resistance, and, therefore, obscure the quantum transport more, thus lowering the threshold. Overall, the lower bound for perfect quantization is taken to be roughly  $N_{2D} \approx 10^{10} \text{ cm}^{-2}$ . Plotted in Figure 3c-d is  $N_{2D}$  vs  $\Delta$  for this lower limit as well as larger values. Realizing quantized transport at room temperature would require a magnetic gap of nearly 0.3 eV, which in terms of magnetic transitions corresponds to Curie temperatures well over 1000 K. Such temperatures are very unlikely for intrinsic systems, yet maybe possible for heterostructures with ferromagnetic insulators such as  $\text{Y}_3\text{Fe}_5\text{O}_{12}$  (YIG), which has a magnetic transition around 560 K. However, for the current TIs the magnetic gap would have to be the same as the bulk band gap, making this again unlikely to be possible at room temperature; nevertheless, it is well within the bounds of liquid nitrogen temperatures, especially considering heterostructures with high-temperature ferromagnets where gaps have been calculated in the range of 0.04-0.1eV<sup>27,28</sup>.

Our results give realistic temperatures for the upper limit where topological states may dominate the electrical response of a material. This upper temperature depends on simple material parameters that are related to basic aspects of the materials chemistry, which can be used to find systems that may operate at elevated temperatures and could be as high as room temperature:

Concerning 3D TIs: for the 2D TSS to dominate the transport requires (1) *larger band gaps*, (2) *smaller dielectric constants*, and (3) *higher effective masses*. This is succinctly captured in Figure 2c, where, for example, current materials with  $E_G < 0.3 \text{ eV}$  and  $\epsilon > 100$ , can be achieved by either reducing  $\epsilon$  to below 50 or increasing the bandgap to larger than 0.6 eV. Finding new materials with such improved properties is, however, a challenge since these parameters are strongly tied to the topological properties. Therefore, a careful balance is needed, as discussed next for each parameter individually.

(1) *Larger band gaps*. To find materials with larger bandgap requires larger mismatch in electronegativity<sup>15</sup>. This is demonstrated for  $\text{Bi}_2\text{Te}_3$  and  $\text{Sb}_2\text{Te}_3$ , whose band gaps are narrower than  $\text{Bi}_2\text{Se}_3$  and the ternary and quaternary tetradymites involving S; this however, simultaneously, pushes the materials towards a topologically trivial phase. This is shown in Figure 2c, where, once band inversion is destabilized,

the band gap rapidly opens, which is explicitly clear for the mixture  $\text{Bi}_2\text{Se}_2\text{S}$ , which has a band gap  $>1$  eV. This implies that  $\text{Bi}_2\text{Se}_3$  is right on the edge of being non-topological. This poses the question: is there a fundamental maximum for band gaps of TIs?

(2) *Smaller dielectric constants.* Reducing the dielectric constant would increase the critical density at which the bulk states would contribute to the overall conductivity. For example, as shown in Figure 2c, with a bandgap of 0.3 eV, reducing the dielectric constant by a factor of two or better, to below 50, will significantly boost  $N_D$ , and thus enable room temperature dominance of the TSS. Achieving such improvements can be accomplished by considering the factors that determine the dielectric response of a material<sup>29</sup>. (1) *Electronic polarizability* due to the displacement of the electron cloud relative to the nuclei. Therefore, atoms with larger electron density have higher polarizabilities, so materials with heavy elements like Bi tend to have high dielectric constants. This can be seen in the tetradymite TIs where  $\text{Bi}_2\text{Te}_3$  has a dielectric constant that is nearly twice that of  $\text{Bi}_2\text{Se}_3$ <sup>16</sup>. This highlights that materials that are likely topological will likely have large dielectric constants, and, thus, low  $N_D$ . Comparing  $\text{Bi}_2\text{Se}_3$  to  $\text{Bi}_2\text{Se}_2\text{S}$  and  $\text{Bi}_2\text{S}_3$ , however, shows only a minimal reduction in dielectric constant, which may indicate there exists a lower bound of  $\epsilon \approx 100$ , for materials that are close to band inversion. (2) *Ionic polarizability* results from shifts in the cation and anion positions due to their net charge, and, therefore, the more ionic the bond the higher the dielectric constant. This is, however, not likely to be a major concern since compounds that favor the narrow band gaps necessary for band inversion are typically covalent (ionic materials tend to have larger gaps). More covalent character is typically favored in the p-block of the periodic table; as discussed below, this simultaneously favors lower effective masses. (3) *Dipole polarizability* occurs when a preexisting dipole changes its orientation in the presence of an electric field. In solids, these are either ferroelectrics or in close proximity to ferroelectricity, and are typically rare, and should be avoided for TIs. Overall, the dielectric constant should be as small as possible ( $\epsilon < 50$ ) for boosting the temperature where the TSS dominate, which can be achieved by reducing the masses of the elements used but maintaining their covalent character.

(3) *Higher effective mass.* Boosting effective mass tends to both raise  $N_D$  while lowering the temperature where the bulk states start contributing to transport (as shown in Figure 2b and c). Since  $N_D$  scales as  $m^{*3}$ , this dominates the overall dependence on  $m^*$ , and, therefore, the larger  $m^*$  leads to better performance of TIs towards the room temperature limit. This can be clearly seen in Figure 2c, where increasing  $m^*$  expands the regime where TSS dominate transport to lower band gaps and larger dielectric constants. Larger  $m^*$  can be achieved by reducing the orbital overlap, which, for example, requires atoms with more localized orbitals. Typically, the *d*- and *f*-orbitals are the most spatially localized, which gives rise to larger effective masses in comparison to the p- and s-orbitals. Further, the heavier the elements are the more delocalized their orbitals and the smaller  $m^*$  becomes. This again places a limitation on TIs since

they are typically observed in *p*-block elements with strong covalency, and, therefore, small effective masses. Searching for new TIs with 3d elements may produce larger  $m^*$ , but, as discussed above, the bonds there tend to be more ionic, which both compromises band inversion while raising the ionic contribution to the dielectric constant; the former point has been well explored in the context of magnetic doping the tetradymites<sup>10,30,31</sup>. This highlights that new materials are needed, but a careful balance among many parameters is required to boost the maximum temperature for surface dominated transport.

Concerning QAHI: the results suggest observing quantized transport near room temperature will be very challenging, though certainly not impossible. In particular, to raise the temperature of the QAHI by utilizing the current materials paradigm of (1) taking a 3D TI, (2) reducing the thickness, and (3) either interfacing it with a magnetic insulator or doping it to be magnetic<sup>10</sup> will require dramatic improvement to both the bulk material as well as the magnetic phase. In particular, the bulk band gap may need to be  $>0.6$  eV with magnetic gap  $>0.3$  eV. As this is unlikely with current materials, this is a direct call for the continued development of dramatically different material paradigms<sup>32–36</sup>. Despite the challenge for pushing to room temperature, near liquid nitrogen temperatures may be within reach of current systems. This would be significantly improved over the current materials with maximum temperatures of 2-6 K<sup>10,32,37</sup>. Since the band gaps of the  $(\text{Bi}_{1-x}\text{Sb}_x)_2\text{Te}_3$  and newly discovered  $\text{MnBi}_2\text{Te}_4$  are of order of 0.15 meV, the transition into a bulk metallic phase should occur near 75 K, which leaves the question of whether the magnetic gap can be increased, through either doping or heterostructuring. Given the extensive amount of work done, magnetic doping to open such a large gap is, again, unlikely, but interfacing such TIs with large-transition-temperature-ferromagnets should be a fruitful route to boosting the temperature up to this limit.

To conclude, we have established simple criteria for the upper limit to observe transport dominated by the topological states, which is a key requirement to realize any topological electronics. The limiting factor is the density of thermally induced carriers. Although this shows that room temperature dominance of either the 2D TSS in a 3D TI or the QAHI are not possible with current materials, discovering new paradigms will likely enable this. Key parameters are increasing band gap (or the magnetic gap for the QAHI), reducing dielectric constant, and increasing effective mass. Each of these are all effective tuning parameters. Specifically, operation at room temperature of a 3D TI can be achieved with a bulk band gap of around 0.6 eV, twice as large as the current materials; alternatively, the dielectric constant must be reduce below at least 50 with a band gap of 0.3 eV. General trends across the periodic table will be useful for finding new materials, but highlight that a subtle balance is required as modulating these parameters can simultaneously jeopardize the topological properties. For example, going from heavy *p*-block elements to lighter elements in the *d*-block may give rise to larger band gaps, reduce contribution of the electronic polarizability to the dielectric constant, and create larger effective mass. Yet, caution must be taken as these may compromise band inversion and increase the ionic polarization contribution to the dielectric constant.

Most excitingly, however, the combination of these parameters are calculatable with first principles methods, and, therefore, may be incorporated to parse databases of known and theorized topological materials<sup>38</sup>. This should enable narrowing down possible candidate materials for synthesis and characterization. As one of the ultimate goals of materials physics is to present new materials with novel functionality for possible applications, the current work gives clear parameters for finding topological materials that could conceivably be used at room temperature for new technologies.

## **Acknowledgments**

This work was supported by the U.S. Department of Energy (DOE), Office of Science, Basic Energy Sciences, Materials Sciences and Engineering Division. We wish to thank Jason Lapano, Joon Sue Lee, Seongshik Oh, Panchapakesan Ganesh, Brian Sales and T. Zac Ward for insightful discussion, and T. Zac Ward for encouragement to publish this work.

## References

- <sup>1</sup> M.Z. Hasan and C.L. Kane, *Rev. Mod. Phys.* **82**, 3045 (2010).
- <sup>2</sup> X.-L. Qi and S.-C. Zhang, *Rev. Mod. Phys.* **83**, 1057 (2011).
- <sup>3</sup> K. v Klitzing, G. Dorda, and M. Pepper, *Phys. Rev. Lett.* **45**, 494 (1980).
- <sup>4</sup> D.J. Thouless, M. Kohmoto, M.P. Nightingale, and M. den Nijs, *Phys. Rev. Lett.* **49**, 405 (1982).
- <sup>5</sup> C.L. Kane and E.J. Mele, *Phys. Rev. Lett.* **95**, 226801 (2005).
- <sup>6</sup> M. König, S. Wiedmann, C. Brüne, A. Roth, H. Buhmann, L.W. Molenkamp, X.-L. Qi, and S.-C. Zhang, *Science* (80-. ). **318**, 766 (2007).
- <sup>7</sup> F.D.M. Haldane, *Phys. Rev. Lett.* **61**, 2015 (1988).
- <sup>8</sup> C.-Z. Chang, J. Zhang, X. Feng, J. Shen, Z. Zhang, M. Guo, K. Li, Y. Ou, P. Wei, L.-L. Wang, Z.-Q. Ji, Y. Feng, S. Ji, X. Chen, J. Jia, X. Dai, Z. Fang, S.-C. Zhang, K. He, Y. Wang, L. Lu, X.-C. Ma, and Q.-K. Xue, *Science* (80-. ). **340**, 167 (2013).
- <sup>9</sup> C.-X. Liu, S.-C. Zhang, and X.-L. Qi, *Annu. Rev. Condens. Matter Phys.* **7**, 301 (2016).
- <sup>10</sup> K. He, Y. Wang, and Q.-K. Xue, *Annu. Rev. Condens. Matter Phys.* **9**, 329 (2018).
- <sup>11</sup> J.E. Moore and L. Balents, *Phys. Rev. B* **75**, 121306 (2007).
- <sup>12</sup> M. Sato and Y. Ando, *Reports Prog. Phys.* **80**, 076501 (2017).
- <sup>13</sup> M. He, H. Sun, and Q.L. He, *Front. Phys.* **14**, (2019).
- <sup>14</sup> Y. Fan and K.L. Wang, *SPIN* **6**, (2016).
- <sup>15</sup> R.J. Cava, H. Ji, M.K. Fuccillo, Q.D. Gibson, and Y.S. Hor, *J. Mater. Chem. C* **1**, 3176 (2013).
- <sup>16</sup> J.P. Heremans, R.J. Cava, and N. Samarth, *Nat. Rev. Mater.* **2**, 1 (2017).
- <sup>17</sup> N. Koirala, M. Brahlek, M. Salehi, L. Wu, J. Dai, J. Waugh, T. Nummy, M.-G. Han, J. Moon, Y. Zhu, D. Dessau, W. Wu, N.P. Armitage, and S. Oh, *Nano Lett.* **15**, 8245 (2015).
- <sup>18</sup> M. Brahlek, N. Koirala, M. Salehi, N. Bansal, and S. Oh, *Phys. Rev. Lett.* **113**, 026801 (2014).
- <sup>19</sup> M. Brahlek, N. Koirala, N. Bansal, and S. Oh, *Solid State Commun.* **215**, 54 (2014).
- <sup>20</sup> P. Syers and J. Paglione, *Phys. Rev. B* **95**, 045123 (2017).
- <sup>21</sup> S.K. Kushwaha, I. Pletikovic, T. Liang, A. Gyenis, S.H. Lapidus, Y. Tian, H. Zhao, K.S. Burch, J. Lin, W. Wang, H. Ji, A. V. Fedorov, A. Yazdani, N.P. Ong, T. Valla, and R.J. Cava, *Nat. Commun.* **7**, 1 (2016).
- <sup>22</sup> P.P. Edwards and M.J. Sienko, *Acc. Chem. Res.* **15**, 87 (1982).
- <sup>23</sup> D.K. Schroder, *Semiconductor Material and Device Characterization*, 3rd ed. (Wiley-IEEE Press, 2015).
- <sup>24</sup> A. Bansil, H. Lin, and T. Das, *Rev. Mod. Phys.* **88**, 1 (2016).
- <sup>25</sup> E. Abrahams, P.W. Anderson, D.C. Licciardello, and T. V. Ramakrishnan, *Phys. Rev. Lett.* **42**, 673 (1979).
- <sup>26</sup> J. Zhang, C.-Z. Chang, Z. Zhang, J. Wen, X. Feng, K. Li, M. Liu, K. He, L. Wang, X. Chen, Q.-K. Xue, X. Ma, and Y. Wang, *Nat Commun* **2**, 574 (2011).
- <sup>27</sup> K.F. Garrity and D. Vanderbilt, *Phys. Rev. B - Condens. Matter Mater. Phys.* **90**, 121103 (2014).

- <sup>28</sup> H. Fu, C.X. Liu, and B. Yan, *Sci. Adv.* **6**, eaaz0948 (2020).
- <sup>29</sup> S. Trolier-McKinstry and R.E. Newnham, *Materials Engineering Bonding, Structure, and Structure-Property Relationships* (Cambridge University Press, Cambridge, 2018).
- <sup>30</sup> J. Moon, J. Kim, N. Koirala, M. Salehi, D. Vanderbilt, and S. Oh, *Nano Lett.* **19**, 3409 (2019).
- <sup>31</sup> J. Zhang, C.Z. Chang, P. Tang, Z. Zhang, X. Feng, K. Li, L.L. Wang, X. Chen, C. Liu, W. Duan, K. He, Q.K. Xue, X. Ma, and Y. Wang, *Science* (80-. ). **340**, 1582 (2013).
- <sup>32</sup> Y. Deng, Y. Yu, M.Z. Shi, Z. Guo, Z. Xu, J. Wang, X.H. Chen, and Y. Zhang, *Science* (80-. ). **367**, 895 (2020).
- <sup>33</sup> M. Serlin, C.L. Tschirhart, H. Polshyn, Y. Zhang, J. Zhu, K. Watanabe, T. Taniguchi, L. Balents, and A.F. Young, *Science* (80-. ). **367**, 900 (2020).
- <sup>34</sup> R. Nandkishore and L. Levitov, *Phys. Rev. B - Condens. Matter Mater. Phys.* **82**, 115124 (2010).
- <sup>35</sup> W.K. Tse, Z. Qiao, Y. Yao, A.H. MacDonald, and Q. Niu, *Phys. Rev. B - Condens. Matter Mater. Phys.* **83**, 155447 (2011).
- <sup>36</sup> M.M. Otrokov, T. V. Menshchikova, M.G. Vergniory, I.P. Rusinov, A.Y. Vyazovskaya, Y.M. Koroteev, G. Bihlmayer, A. Ernst, P.M. Echenique, A. Arnau, and E. V Chulkov, *2D Mater.* **4**, 025082 (2017).
- <sup>37</sup> M. Mogi, R. Yoshimi, A. Tsukazaki, K. Yasuda, Y. Kozuka, K.S. Takahashi, M. Kawasaki, and Y. Tokura, *Appl. Phys. Lett.* **107**, 182401 (2015).
- <sup>38</sup> B. Bradlyn, L. Elcoro, J. Cano, M.G. Vergniory, Z. Wang, C. Felser, M.I. Aroyo, and B.A. Bernevig, *Nature* **547**, 298 (2017).
- <sup>39</sup> P. Enders and R. Schuchardt, *Phys. Status Solidi* **135**, 207 (1986).
- <sup>40</sup> B. Lenoir, M. Cassart, J.P. Michenaud, H. Scherrer, and S. Scherrer, *J. Phys. Chem. Solids* **57**, 89 (1996).
- <sup>41</sup> L.S. Lerner, K.F. Cuff, and L.R. Williams, *Rev. Mod. Phys.* **40**, 770 (1968).
- <sup>42</sup> D.M. Korn and R. Braunstein, *Phys. Rev. B* **5**, 4837 (1972).
- <sup>43</sup> X. Chen, D. Parker, and D.J. Singh, *Sci. Rep.* **3**, 1 (2013).
- <sup>44</sup> C.L. Mitsas and D.I. Siapkas, *Solid State Commun.* **83**, 857 (1992).
- <sup>45</sup> H. Lin, R.S. Markiewicz, L.A. Wray, L. Fu, M.Z. Hasan, and A. Bansil, *Phys. Rev. Lett.* **105**, 036404 (2010).
- <sup>46</sup> D. Coquillat, A. Pradel, G. Brun, and J.C. Tedenac, *Phys. Status Solidi* **82**, 295 (1984).
- <sup>47</sup> Y.L. Chen, Z.K. Liu, J.G. Analytis, J.H. Chu, H.J. Zhang, B.H. Yan, S.K. Mo, R.G. Moore, D.H. Lu, I.R. Fisher, S.C. Zhang, Z. Hussain, and Z.X. Shen, *Phys. Rev. Lett.* **105**, 266401 (2010).
- <sup>48</sup> M. Neupane, S.Y. Xu, L.A. Wray, A. Petersen, R. Shankar, N. Alidoust, C. Liu, A. Fedorov, H. Ji, J.M. Allred, Y.S. Hor, T.R. Chang, H.T. Jeng, H. Lin, A. Bansil, R.J. Cava, and M.Z. Hasan, *Phys. Rev. B - Condens. Matter Mater. Phys.* **85**, 235406 (2012).
- <sup>49</sup> O. Madelung, *Semiconductor Data Handbook* (Springer, Berlin, 2004).
- <sup>50</sup> J. Grigas, J. Meshkauskas, and A. Orliukas, *Phys. Status Solidi* **37**, K39 (1976).
- <sup>51</sup> P. Lošćák, J. Horák, and R. Novotný, *Phys. Status Solidi* **131**, K67 (1985).
- <sup>52</sup> H. Ji, J.M. Allred, M.K. Fuccillo, M.E. Charles, M. Neupane, L.A. Wray, M.Z. Hasan, and R.J. Cava,

**Figures**  
**Figure 1**

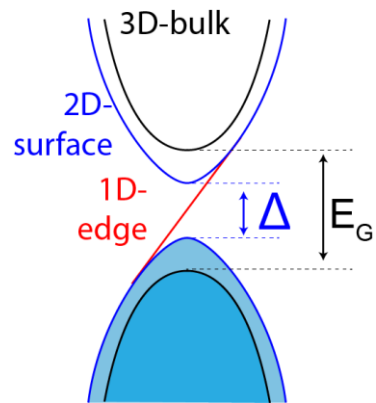


**Figure 1** Schematic of generic topological band structures used for the calculations where  $E_G$  is the bulk band gap, and  $\Delta$  is the magnetic gap in the 2D-topological surface states

**Figure 2**

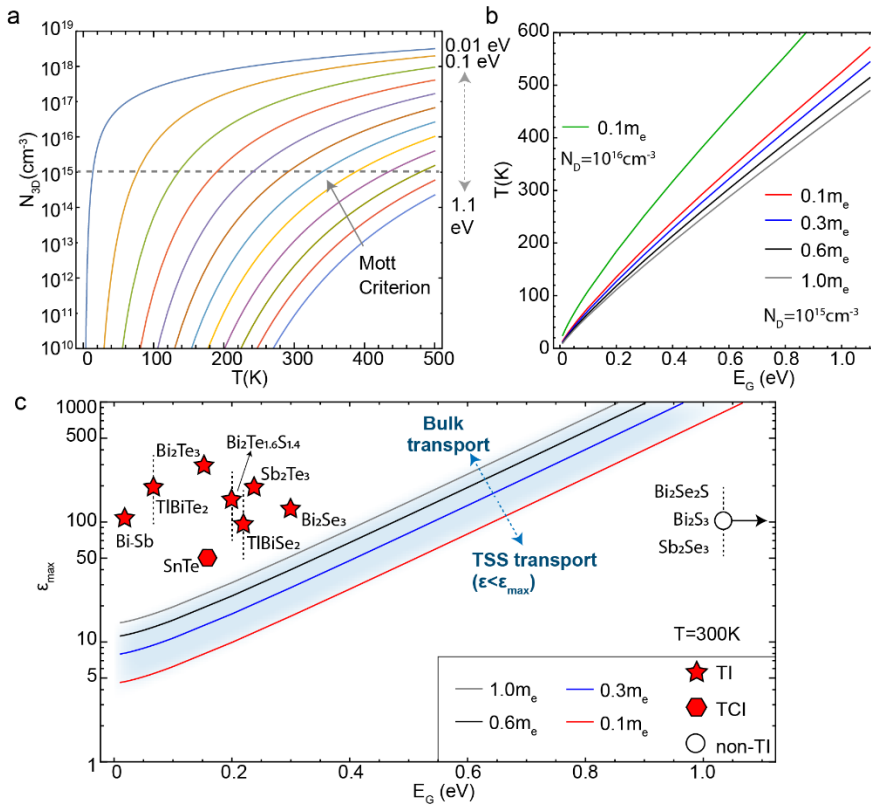


**Figure 2.** (a) Temperature dependence of the thermal induced carrier density compared to the Mott criterion for various bandgaps with  $m^* = 0.1m_e$ . The curves correspond to bandgaps 0.01 eV (top) then 0.1-1.1 eV in steps of 0.1 eV. (b) Bandgap versus temperature where the curves in (a) intersect the Mott criterion, as indicated. (c) Bandgap versus maximum dielectric constant for various effective masses with  $T = 300$  K. The symbols represent known topological materials (filled symbol) and non-TIs (open symbol). For the topological surface states (TSS) to dominate transport at room temperature they must fall below the  $\epsilon_{Max}$  vs  $E_G$  curves, as indicated. When the dielectric constant was not well-studied, a vertical dashed line is used to indicate the range of possible values. Data for select materials was from references 15,16,47–52,39–46.

**Figure 3**

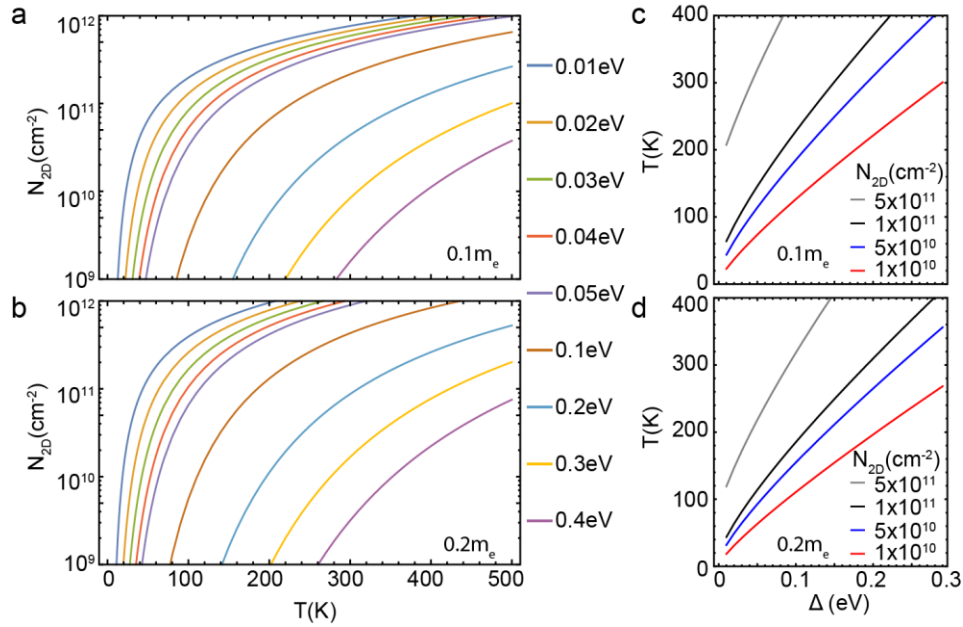


**Figure 3** (a-b) Temperature dependence of the 2D carrier concentration for various bandgaps with  $m^* = 0.1m_e$  (a) and  $m^* = 0.2m_e$  (b). (c-d) Magnetic gap versus temperature where the curves in (a-b) intersect the carrier concentrations of  $1 \times 10^{10}$  cm<sup>-2</sup>,  $5 \times 10^{10}$  cm<sup>-2</sup>,  $1 \times 10^{11}$  cm<sup>-2</sup>, and  $5 \times 10^{11}$  cm<sup>-2</sup>, as indicated.